

FR-7974

**Motion Stability Measurements of a Submarine-Towed
ELF Receiving Platform**

**Robert J. Dinger
Joseph Goldstein**

April 23 , 1976

Naval Research Laboratory

SECURITY CLASSIFICATION OF THIS PAGE (When Data Entered)

REPORT DOCUMENTATION PAGE		READ INSTRUCTIONS BEFORE COMPLETING FORM
1. REPORT NUMBER NRL Report 7974	2. GOVT ACCESSION NO.	3. RECIPIENT'S CATALOG NUMBER
4. TITLE (and Subtitle) MOTION STABILITY MEASUREMENTS OF A SUBMARINE-TOWED ELF RECEIVING PLATFORM	5. TYPE OF REPORT & PERIOD COVERED Interim report on one phase of a continuing NRL Problem	
	6. PERFORMING ORG. REPORT NUMBER	
7. AUTHOR(s) Robert J. Dinger and Joseph Goldstein	8. CONTRACT OR GRANT NUMBER(s)	
9. PERFORMING ORGANIZATION NAME AND ADDRESS Naval Research Laboratory Washington, D.C. 20375	10. PROGRAM ELEMENT, PROJECT, TASK AREA & WORK UNIT NUMBERS NRL Problem R07-34 Project XF21-222-035	
11. CONTROLLING OFFICE NAME AND ADDRESS Naval Electronic Systems Command Washington, D.C. 20375	12. REPORT DATE April 23, 1976	
	13. NUMBER OF PAGES 17	
14. MONITORING AGENCY NAME & ADDRESS (if different from Controlling Office)	15. SECURITY CLASS. (of this report) Unclassified	
	15a. DECLASSIFICATION, DOWNGRADING SCHEDULE	
16. DISTRIBUTION STATEMENT (of this Report) Approved for public release; distribution unlimited.		
17. DISTRIBUTION STATEMENT (of the abstract entered in Block 20, if different from Report)		
18. SUPPLEMENTARY NOTES		
19. KEY WORDS (Continue on reverse side if necessary and identify by block number) SQUID ELF communications SANGUINE ELF antennas		
20. ABSTRACT (Continue on reverse side if necessary and identify by block number) The design and ultimate performance of an extremely low frequency (ELF) supercon- ducting quantum interference device (SQUID) antenna that is mounted in a submarine-towed buoy depends critically on the motion spectrum of the buoy. Motion spectrum measurements from nearly direct current to 100 Hz were conducted on a hydrodynamically stabilized buoy while being towed in the 650-m towing basin of the David Taylor Naval Ship Research and (Continued)		

DD FORM 1473
1 JAN 73

EDITION OF 1 NOV 65 IS OBSOLETE
S/N 0102-014-6601

SECURITY CLASSIFICATION OF THIS PAGE (When Data Entered)

Development Center, Carderock, Md. The spectra show that the angular motion of the buoy can be held to 10^{-6} rad or less within the ELF receiver bandwidth of 30 to 130 Hz, as long as properly streamlined fairings are used on the hydrofoil trailing edges to prevent oscillations from vortex shedding. Low frequency oscillations of the buoy were 10^{-3} rad or less for frequencies down to 0.025 Hz. This performance of the buoy is sufficient to permit it to serve as a towed platform for the NRL prototype SQUID receiver.

CONTENTS

INTRODUCTION	1
DESCRIPTION OF TOW TESTS	3
RESULTS	5
Rate Gyro Data	5
Accelerometer Data	7
APPLICATION OF RESULTS TO SQUID ELF ANTENNA DESIGN	11
CONCLUSIONS	13
ACKNOWLEDGMENTS	13
REFERENCES	13

MOTION STABILITY MEASUREMENTS OF A SUBMARINE-TOWED ELF RECEIVING PLATFORM

INTRODUCTION

The ability to communicate with submarines at operational depth is of prime importance to the U.S. Navy. Present long-range submarine communication systems operate in the very-low-frequency (VLF) band (3 to 30 kHz), which requires the receiving antennas to be relatively near the ocean surface. A communication system operating in the extremely-low-frequency (ELF) band (30 to 300 Hz) would allow reception at a submarine's operational depth because of the greatly increased penetration at ELF frequencies of electromagnetic waves below the surface of the ocean. To achieve omnidirectionality in the ELF band, efforts have been concentrated on the development of an E-field sensing trailing-wire antenna with distributed electrodes [1] and an H-field-sensing ferromagnetic-core solenoid [2], both of which would be towed behind a submarine as a complementary pair. The E-field trailing-wire antenna has been shown to have a noise level that meets the required sensitivity specification; however, to date, the H-field solenoid self-noise level is nearly 20 dB above the required sensitivity, and further improvements in self-noise level may not be possible. Because the trailing-wire E-field antenna alone is not omnidirectional, an alternative antenna is required.

The use of a Josephson junction detector in the form of a superconducting quantum interference device (SQUID) [3] shows promise for overcoming these limitations. The SQUID is an extremely sensitive H-field vector sensor that has been shown to satisfy the noise requirements for reception of an ELF signal below the surface by the use of a pickup coil that is only 5 cm in diameter. To achieve the desired omnidirectionality, three SQUIDs can be arranged in a mutually orthogonal configuration.

The three SQUID sensors must be mounted in a long-hold-time, liquid helium dewar to maintain the necessary superconducting temperature. Mounting the sensors on the hull may result in excessive interference from submarine-generated magnetic fields. Consequently, we are investigating the possibility of mounting the antenna on a buoy that can be towed up to 100 m behind the submarine.

The motion of the buoy, however, creates noise because the SQUID is a vector sensor required to detect a signal of 10^{-14} Tesla (T), while operating in the earth's magnetic field (H_e) of 6×10^{-5} T. The motion of the towed buoy will modulate H_e and result in an AC noise field at the motion frequencies. The motion-induced variations that occur within the ELF receiver bandwidth of 30 to 130 Hz will constitute a major source of noise and must be removed by suitable signal processing. In addition, the motion-induced noise must be sufficiently low so that the dynamic range of the SQUID output electronics is not exceeded.

The motion spectrum of the ELF towed buoy thus greatly influences the design of both the SQUID electronics and signal processor. The feasibility of a SQUID ELF antenna may rely on the availability of a towed buoy of sufficient stability.

To determine the system parameters influenced by motion of the buoy, we compiled motion spectra on a towed buoy that was generally considered to be the most stable hydrodynamically of any communications buoy designed to date. This buoy (Fig. 1) was designed and constructed in 1972 by the David W. Taylor Naval Ship Research and Development Center (DTNSRDC), Bethesda, Md. It is experimental and was specifically designed to be very stable. A full description of the buoy can be found in Ref. 4.

In November 1974, the buoy was taken to the DTNSRDC towing basin. This report presents the results of the towing tests conducted on the buoy at that time and discusses the implications of these results on the SQUID ELF antenna design. This work has been summarized in Ref. 5.

These tests were intended to predict the performance of the buoy when towed at sea behind a submarine. The limitations of towing basin measurements for predicting sea performance are probably obvious, but they should be mentioned. The influence of ocean disturbances such as currents and swells and the ability of the buoy to recover from such disturbances cannot be determined from basin measurements. The effect of wake disturbances from the submarine also cannot be determined. In this regard, however, the buoy tested here was designed with high lift hydrofoils that position it well above the wake of the submarine while being towed. Potentially, the greatest uncertainty in predicting sea performance is the instability that can occur when a buoy is towed at the end of a long cable. Large-amplitude yawing instabilities, as described by Païdoussis [6], can occur in buoys towed with certain "resonant" cable lengths. Previous sea trials [4] of this test buoy revealed no such instabilities greater than the $\pm 5 \times 10^{-3}$ -rad noise level of the sensors used in those trials. However, the sea trials described in Ref. 4 were somewhat limited in their scope, and it is conceivable that long cables will produce motion excursions that exceed the amplitudes measured in the tests described in this report.

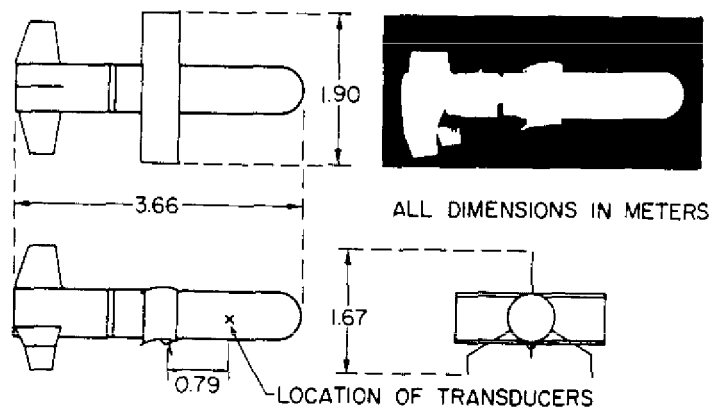


Fig. 1—The tested buoy

DESCRIPTION OF TOW TESTS

The buoy was instrumented with a triaxial rate gyroscope and a triaxial linear accelerometer mounted at the point shown in Fig. 1. The triaxial rate gyroscope (manufactured by Humphrey, Inc., Model RT02-0201-1) was selected for its high sensitivity, which is approximately 0.2 mrad/s. The triaxial linear accelerometer (manufactured by Endevco, Inc., Model 2228C) was of a standard design with an output voltage sensitivity of $6 \mu\text{V}/(\text{cm}/\text{s}^2)$. The outputs of these sensors were amplified, filtered, and recorded on analog and digital magnetic tape.

The buoy was towed in a 650-m towing basin as shown diagrammatically in Fig. 2. When towed in the ocean by a submarine, the buoy is towed from below and is positively buoyant. However, because the buoy cannot be towed from below in the towing basin without excessively disturbing the water, the buoy was made negatively buoyant and was towed in an inverted position from above. Thus, the configuration in Fig. 2 is a mirror image of the configuration used during submarine towing. The vibrational behavior of the buoy is not expected to be altered by this inverted towing position. The buoy was towed at steady speeds of 2 to 7 knots; in addition, several constant-acceleration runs with a top speed of 7 knots were made. Higher speeds were not used because 7 knots was the maximum design speed of the buoy. Each run was repeated three times in order to verify the repeatability of the measurements. The static angle of attack was 3° nose up, 0° , or 3.5° nose down. Because each run was repeated three times and three body trim angles were used, there were at least nine runs at each speed. A total of 80 runs was made for these tests.

The rate gyros were intended to provide coverage of the bandwidth from DC to 20 Hz and the accelerometers from 10 Hz to more than 100 Hz. Because the largest buoy motions are expected to occur at frequencies below several Hertz, it is important that the limitations of the rate gyros at these low frequencies be well understood. Consider the buoy oscillating sinusoidally at a frequency ω with a peak amplitude θ_0 , so that the angular excursion θ of one of the principal axes is given by

$$\theta = \theta_0 e^{i\omega t}. \quad (1)$$

The rate gyro sensitive to this axis will produce an output proportional to

$$\dot{\theta} = \omega \theta_0 e^{i(\omega t + \pi/2)}. \quad (2)$$

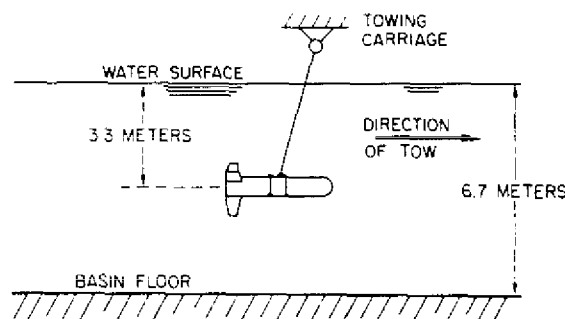


Fig. 2—Towing configuration

At a particular frequency, the *excursion* noise level θ_N is related to the gyro output noise level $\dot{\theta}_N$ by, from Eq. (2),

$$|\theta_N| = \left| \frac{\dot{\theta}_N}{\omega} \right|. \quad (3)$$

The sensitivity of the rate gyro is independent of frequency; hence, as the frequency ω decreases the excursion noise level increases for given $\dot{\theta}_N$. Figure 3 shows Eq. (3) as plotted with the rate gyro manufacturer's nominal value for $\dot{\theta}_N$ of 0.2 mrad/s and excursion noise level increasing at low frequency. Figure 3 shows that the rate gyro cannot resolve very low frequency oscillations of the buoy.

Because the accelerometers measure linear and not angular acceleration, the conversion of their output to angular excursion is somewhat more complicated than the conversion for the rate gyros. Not only must a double integration with respect to time be made, but also an axis about which the rotation is occurring must be either determined or assumed. The first assumption to be made in this regard is that, once the towing carriage

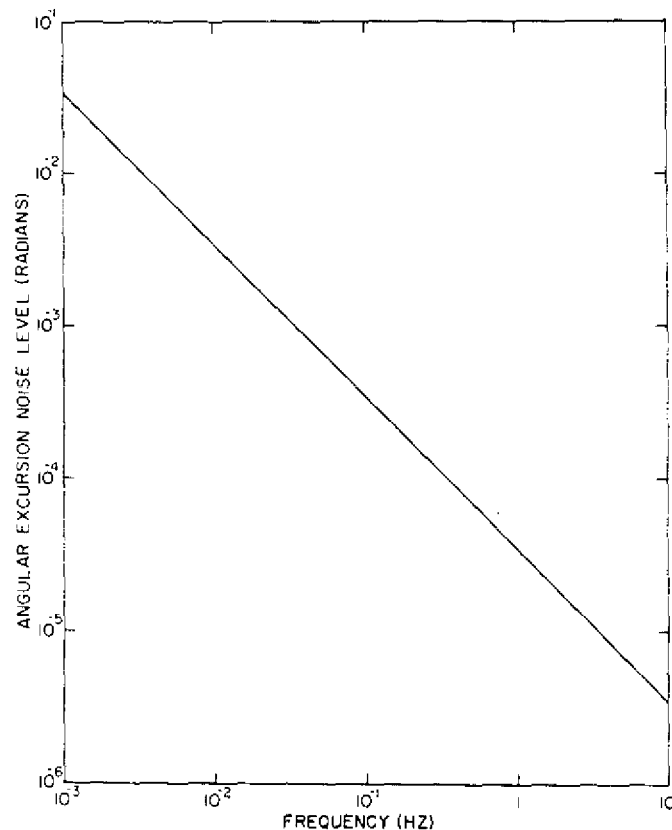


Fig. 3—Variation of rate-gyro excursion noise level as a function of frequency

and buoy reach a steady speed, there is no relative motion of the center of mass of the buoy with respect to the carriage. Second, because the towing point on the buoy is located at its center of gravity, we will assume that the axes of rotation are coincident with the principal axes of the body.* In other words, all motion detected by the accelerometers is assumed to be simple roll, pitch, and yaw motion of the buoy. Hence the angular excursion accelerations $\ddot{\theta}$ are related to the outputs of the linear accelerometers \ddot{X} by

$$\ddot{\theta}_i = \frac{\ddot{X}_i}{\ell_i}, \quad (4)$$

where $i = r, p, y$ for the roll, pitch, and yaw accelerometers, respectively. The quantity ℓ_i is the length of the perpendicular between the accelerometer and the corresponding roll, pitch, or yaw axis. The values of the ℓ_i are $\ell_r = 0$, $\ell_p = 80$ cm, and $\ell_y = 80$ cm. In all of the data, the output of the roll accelerometer (once a steady towing speed was reached) was essentially noise limited, as expected from Eq. (4) for $\ell_r = 0$. This fact also tends to support the assumptions used to derive Eq. (4).

RESULTS

Rate Gyro Data

Figure 4 (a) displays a portion of a strip chart recording of the pitch rate gyro output taken during a 7-knot run. Since the rate gyro produces an output voltage proportional to angular time rate of change, this voltage must be integrated with respect to time in order to obtain the time history of the angular excursion. The trace in Fig. 4 (b) shows the result of integrating the rate gyro output. A fairly regular oscillation of 0.4 mrad with a period of about 2 s can be discerned in this trace. In addition, a large fluctuation of about 1.4 mrad occurs between 10 and 20 s. The frequency of this fluctuation is approximately 0.025 Hz. According to Fig. 3, the noise level at this frequency is about 1 mrad; hence the large fluctuation is simply rate-gyro noise.

To study the spectral content of the motion, we digitized the recorded rate-gyro outputs and used them as input to a standard Fast Fourier Transform (FFT) routine on a digital computer. Figure 5 shows typical spectra of the output of the rate-gyro sensor for the pitch axis at steady state speeds of 4 and 7 knots. A portion of the recorded output for this run is shown in Fig. 4. The spectra show low frequency motions of the body that increase in bandwidth as speed increases. The 4-knot spectrum has a bandwidth extending from near DC to about 2 Hz, while the 7-knot spectrum extends to about 4 Hz. In each case the spectral amplitudes are approximately 6×10^{-4} rad/s, indicating that an increase in speed has essentially no effect on the amplitude of the low frequency motion. The fluctuation with a 2-s period visible in Fig. 4 can be seen as the peak at 0.5 Hz in Fig. 5.

*The principal axes of the body are the eigenvectors of the moment of inertia tensor. In the buoy used in these tests, the principal axes coincide with the usual roll, pitch, and yaw axes.

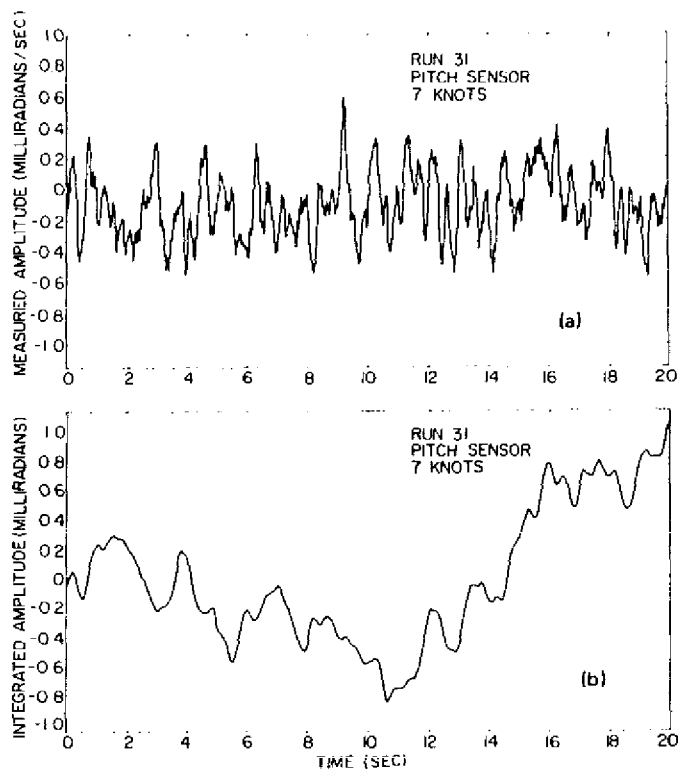


Fig. 4—(a) Real-time output of the pitch rate gyroscope; (b) Time integral of the top trace, displaying pitch angular excursion as a function of time

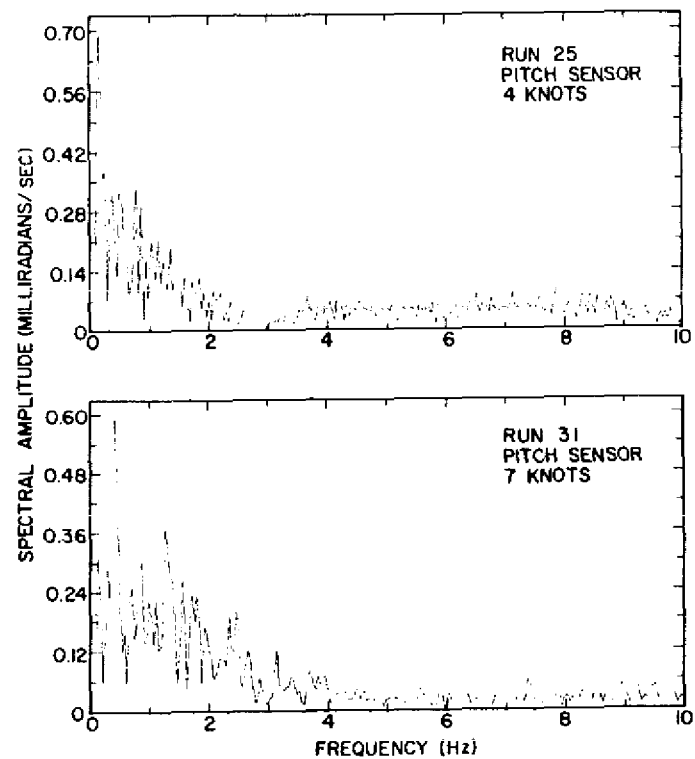


Fig. 5—Spectra of the pitch rate-gyro output for two different towing speeds

Figure 6 displays the spectra of the integrated data from Fig. 5 and represents the pitch angular excursion of the buoy. A sensor resolution curve, similar to the curve plotted in Fig. 3, has been added to Fig. 6 to emphasize that the increasing spectral amplitude at low frequency is in part a result of the increasing sensor noise level at low frequency. These curves of excursion spectra show that the buoy excursions are less than 10^{-3} rad.

Data from the roll and yaw sensors and from runs at other speeds gave results similar to data found in Figs. 4 through 6. The static angle of attack of the buoy was observed to have no effect on the motion spectra for the range ($\pm 3.5^\circ$) studied in these measurements.

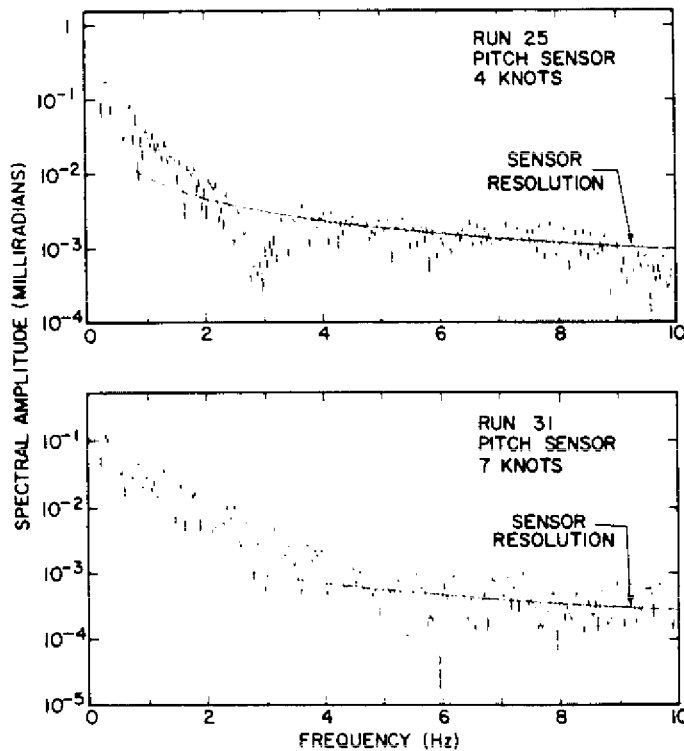


Fig. 6—Spectra of the time integral of the pitch rate-gyro output for two different towing speeds, displaying pitch angular excursion as a function of frequency

Accelerometer Data

Figure 7 displays the spectra of the output of the x-oriented (pitch-sensitive) accelerometer for steady towing speeds of 4 and 7 knots. The prominent feature of these spectra is the presence of two sharp spikes. Figure 8 contains the doubly integrated spectra from Fig. 7, where Eq. (4) has been used to convert linear acceleration to angular excursion. Except for the two spikes and their harmonics, it is evident that the spectra reflect the accelerometer noise level; and the maximum excursions of the buoy are 10^{-6} rad and less.

Fig. 7—Spectra of the x-oriented (pitch-sensitive) accelerometer output for two different towing speeds

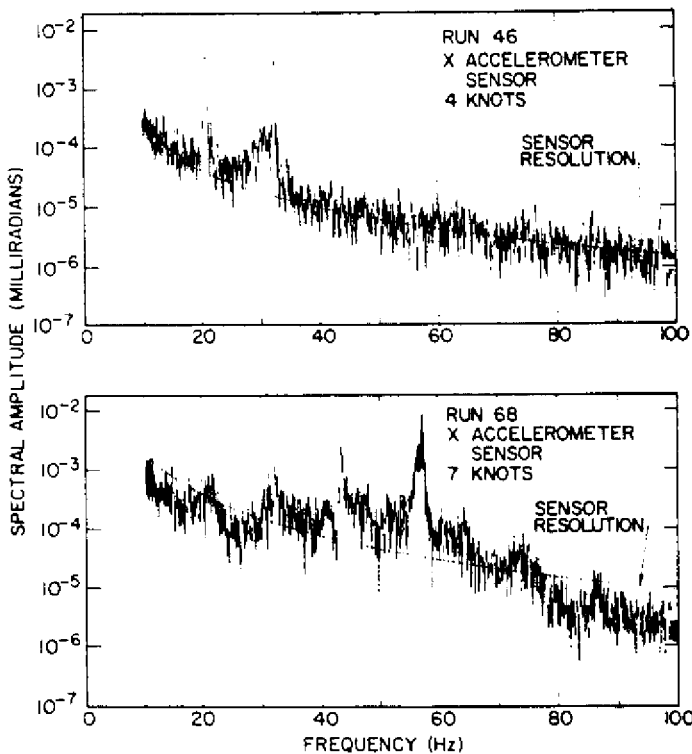
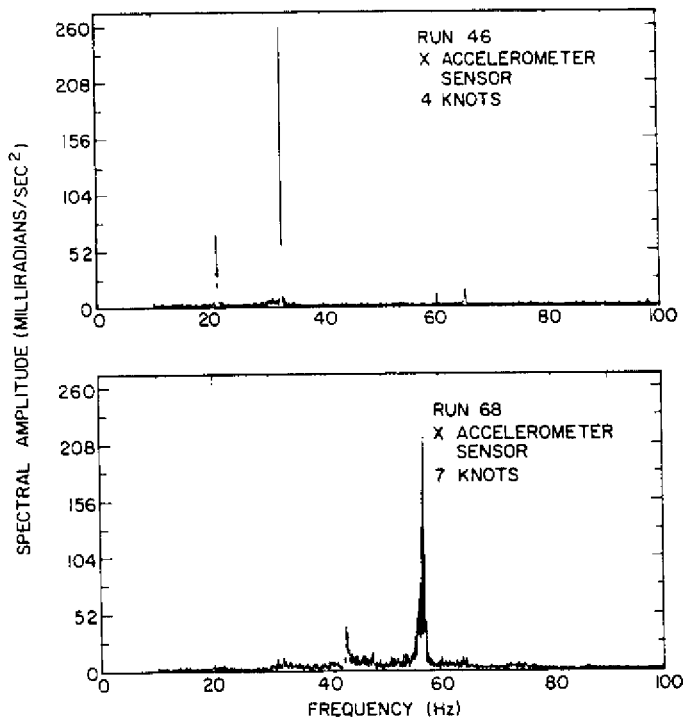


Fig. 8—Spectra of the doubly integrated, pitch-sensitive accelerometer output for two different towing speeds, displaying pitch angular excursion as a function of frequency. Sensor resolution curves, similar in nature to the curve of Fig. 3, are also shown.

The spikes in the accelerometer spectra were seen in both the pitch and yaw accelerometers; the frequencies of the peaks varied approximately linearly with speed. This dependence is shown graphically in Fig. 9, in which the frequency of the peak largest in amplitude is plotted as a function of towing speed. Figure 10 displays a series of spectra from a constant-acceleration run. These spectra were computed on an analog spectrum analyzer with a considerably lower resolution than the digitally computed spectra given in Figs. 7 and 8; thus the peaks appear to be broader. The linear dependence of peak position on speed is clearly evident.

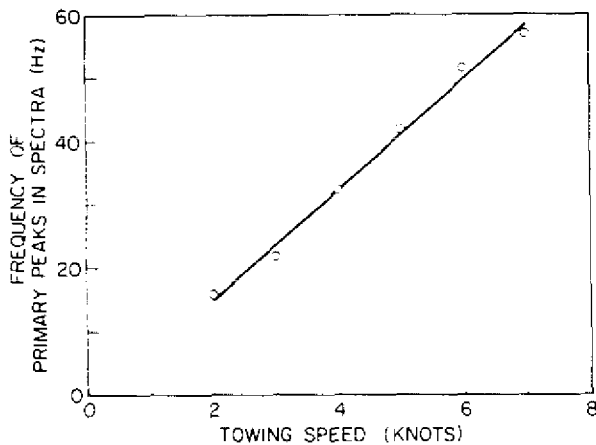


Fig. 9—Variation of frequency of largest spike in x-oriented (pitch-sensitive) accelerometer spectra as a function of towing speed

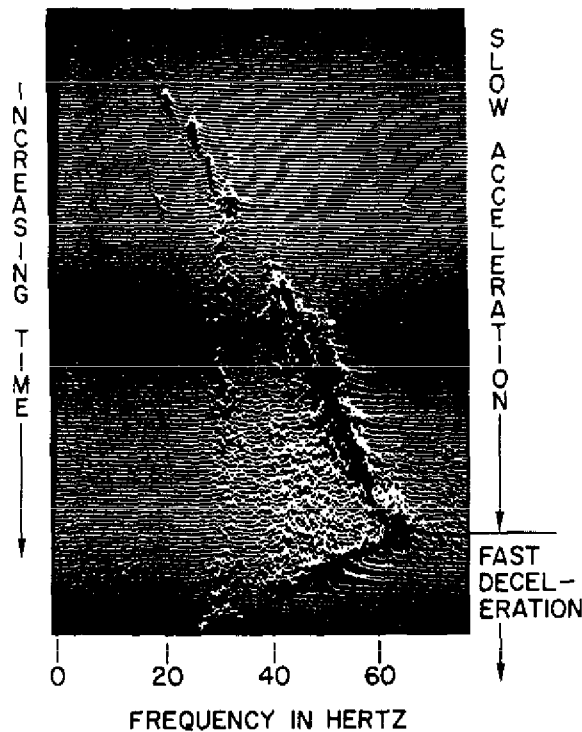


Fig. 10—Spectra of the pitch-sensitive accelerometer output as a function of time for data taken during a constant acceleration run. Peak speed is approximately 7 knots.

The source of these oscillations was traced to the formation of vortices at the blunt trailing edges of the buoy hydrofoils. Vortices form in an alternating manner at the top and bottom edges of the rear of each hydrofoil. These vortices then "peel" away from the edges at a rate dependent on speed through the water and the thickness of the hydrofoil. The turbulence from the vortices couples to the buoy, causing the buoy to oscillate. Two peaks are present because of two different thicknesses of the buoy hydrofoils. This vortex shedding phenomenon is described in detail by Vallentine [7].

To verify that the oscillations were caused by vortex shedding and to determine to what extent proper streamlining can reduce their amplitude, we attached simple fairings constructed of stainless steel shim stock to the rear of some portions of the hydrofoils. Figure 11 shows the buoy with the fairings. A comparison of spectra taken before and after the fairings were added is given in Fig. 12. The streamlining drastically reduces the amplitude of oscillations, the peak at 56 Hz having all but disappeared. The peak at 43 Hz is the result of vortex shedding from the horizontal midbody surfaces to which no fairings were added (see Fig. 11). Thus this peak is still present in the spectra of Fig. 12 (b). We conclude that proper streamlining and fairing of the hydrofoil trailing edges would eliminate the observed spectral peaks entirely.

The peak near 48 Hz in both spectra of Fig. 12, the low amplitude peaks of Fig. 8, and the structure at frequencies of 30 Hz and higher in Fig. 10 probably result from oscillations caused by turbulence from the cylindrical body of the buoy. The structure at 30 Hz in Fig. 10 has an onset at approximately 2 knots. Apparently, an appreciable wake does not form until this speed is attained. None of these oscillations exceed 10^{-6} rad in amplitude.



Fig. 11—Fairings added to the trailing edges of some of the hydrofoils of the buoy

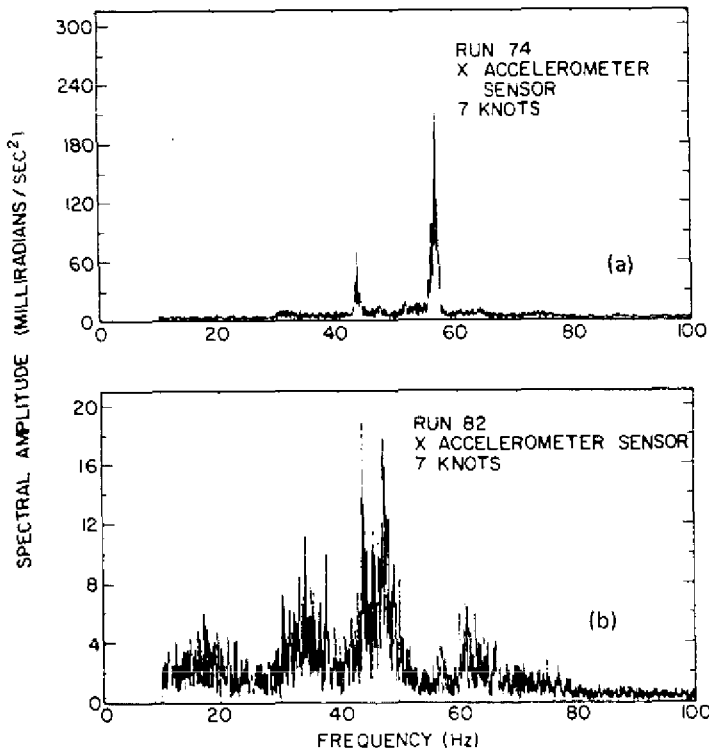


Fig. 12—Comparison of accelerometer spectra taken before (a) and after (b) fairings were added to the trailing edges of the buoy hydrofoils

APPLICATION OF RESULTS TO SQUID ELF ANTENNA DESIGN

The principal constraint that buoy motion places upon the SQUID ELF antenna design is that of dynamic range; that is, the dynamic range must be sufficient to handle the largest motion-induced signal without saturation of the SQUID sensors. Figure 13 shows the required dynamic range as a function of maximum buoy excursion. This graph assumes a noise level of $10^{-14} \text{ T}/\sqrt{\text{Hz}}$ for the sensors and a value of $6 \times 10^{-5} \text{ T}$ for the earth's field. The required dynamic range is determined by the large amplitude motions that occur at very low frequencies. Although the angular rate sensors used here are incapable of accurately determining near DC excursions, as discussed in the section "Description of Tow Tests," it can be estimated from Fig. 6 that the maximum excursions are probably no greater than $5 \times 10^{-4} \text{ rad}$. This value requires a dynamic range of 130 dB, which is within the 140-dB analog dynamic range of the NRL prototype SQUID receiver [5]. The possibility remains that larger motions are present in the buoy that were too low in frequency to be resolved by the rate-gyro sensors.

The signal processing method that has been developed for the removal of residual motion noise determines the components of the earth's magnetic field \vec{H}_e by an adaptive technique and then sums the square of these components in order to remove the earth's field as a large DC component [8]. The accuracy with which the components must be determined is given by the ratio of the desired system noise level to the maximum in-band motion signal. Figure 14 gives the allowable error in the determination of H_e as

Fig. 13—Graph of dynamic range required for SQUID sensors as a function of maximum angular excursion of the buoy

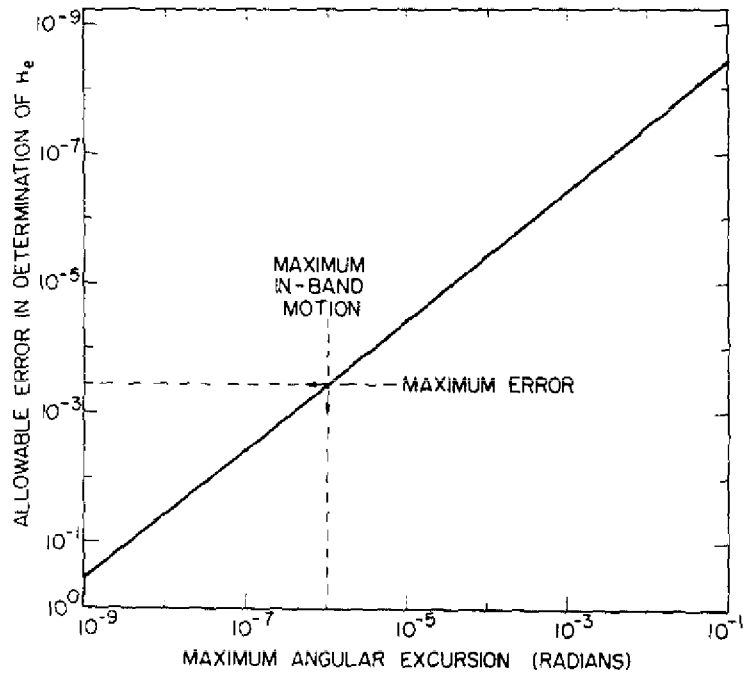
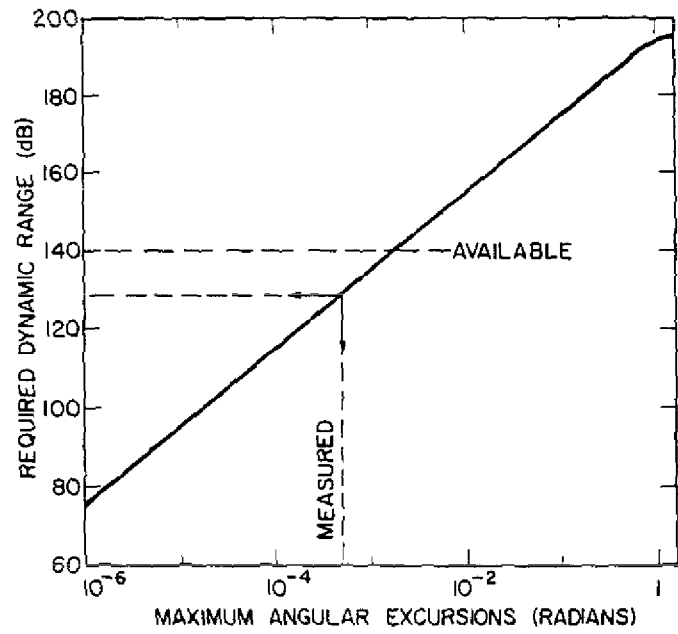


Fig. 14—Variation of allowable error in the determination of the components of the earth's field vector as a function of the maximum in-band (30-130 Hz) angular excursion

a function of the maximum in-band (30-130 Hz) angular excursion. For the maximum excursion of 10^{-6} rad, the components of the earth's field must be determined to an accuracy of less than one part in 10^4 , or approximately 6×10^{-9} T. Such accuracy is obtainable using the adaptive technique described in Ref. 8.

CONCLUSIONS

We have shown that the angular motion of a hydrodynamically stabilized buoy can be held to 10^{-6} rad or less within the ELF receiver bandwidth of 30 to 130 Hz. This level of performance can be obtained if fairings are used on the trailing edges of the buoy hydrofoils. Low frequency oscillations of the buoy were 10^{-3} radians or less for frequencies down to 0.025 Hz. This low level of motion noise was obtained under the ideal conditions of towing basin measurements; some degradation in performance probably can be anticipated when the buoy is actually towed behind a submarine. In general, however, we believe that the angular excursions of the tested buoy are sufficiently low to permit it to serve as a towed platform for the NRL prototype SQUID receiver, if suitable processing of the SQUID outputs is provided to remove the residual motion noise and if fairings are added to the hydrofoils.

ACKNOWLEDGMENTS

We would like to thank Frederick C. Belen, William J. VonFeldt, and Robert M. Brewer of the David W. Taylor Naval Ship Research and Development Center, Carderock, Md., for their assistance during the towing tests.

REFERENCES

1. C. T. Fessenden and D. H. S. Cheng, "Development of a Trailing-Wire E-Field Submarine Antenna for Extremely Low Frequency (ELF) Reception," *IEEE Trans. COM-22*, 428-437 (Apr. 1974).
2. A. D. Cafaro, L. Dalsass, and D. O'Brien, "Stress-Induced Noise in Magnetic-Cored H-Field Antennas," *IEEE Trans. COM-22*, 543-548 (Apr. 1974).
3. S. A. Wolf, J. R. Davis, and M. Nisenoff, "Superconducting Extremely Low Frequency (ELF) Magnetic Field Sensors for Submarine Communications," *IEEE Trans. COM-22* 549-554 (Apr. 1974).
4. C. W. Sieber, "Full-Scale Demonstrations of the Hydrodynamic Performance of the Primary Towed Vehicle System for Project Classic Thicket," Naval Ship Research and Development Center Report 487-H-02, Oct. 1972.
5. J. R. Davis, R. J. Dinger, and J. Goldstein, "Development of a Superconducting ELF Receiving Antenna," NRL Report 7990 (in press).
6. M. P. Païdoussis, "Dynamics of Submerged Towed Cylinders," in *Eighth Symposium on Naval Hydrodynamics*, Pasadena, Calif., Aug. 24-28, 1970, p. 981.

7. H. R. Vallentine, *Applied Hydrodynamics*, 2nd ed., Plenum Press, New York, 1967, p. 267.
8. R. J. Dinger and J. R. Davis, "Adaptive Methods for Motion-Noise Compensation in Extremely Low Frequency Submarine Receiving Antennas," submitted to *IEEE Proceedings*.